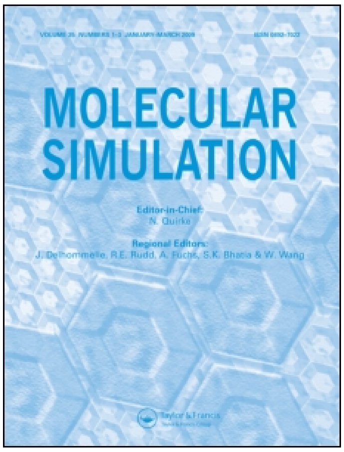

Molecular Simulation
Publication details, including instructions for authors and subscription information:
http://www.informaworld.com/smpp/title~content=t713644482

Molecular Dynamics Simulation Studies of Zeolite-A. IV. Structure and Dynamics of NH_4 ions in a Rigid Dehydrated Zeolite-A

Sang Gu Choi[a]; Song Hi Lee[b]
[a] Department of Industrial Safety, Yangsan Junior College, Yangsan, Korea [b] Department of Chemistry, Kyungsung University, Pusan, Korea

To cite this Article Choi, Sang Gu and Lee, Song Hi(1996) 'Molecular Dynamics Simulation Studies of Zeolite-A. IV. Structure and Dynamics of NH_4 ions in a Rigid Dehydrated Zeolite-A', Molecular Simulation, 17: 2, 113 — 130
To link to this Article: DOI: 10.1080/08927029608024100
URL: http://dx.doi.org/10.1080/08927029608024100

Molecular Simulation, 1996, Vol. 17, pp. 113–130
Reprints available directly from the publisher
Photocopying permitted by licence only

MOLECULAR DYNAMICS SIMULATION STUDIES OF ZEOLITE-A. IV. STRUCTURE AND DYNAMICS OF NH_4^+ IONS IN A RIGID DEHYDRATED ZEOLITE-A.

SANG GU CHOI$^+$ and SONG HI LEE*

Department of Chemistry, Kyungsung University, Pusan Korea 608-736
$^+$Department of Industrial Safety, Yangsan Junior College, Yangsan, Korea 626-800

(Received May 1995, accepted August 1995)

In recent papers [1–3] we reported molecular dynamics simulation studies of ions and water molecules adsorbed in a rigid zeolite-A framework using a simple Lennard-Jones potential plus Coulomb potential with Ewald summation to investigate the structure and dynamics of the adsorbates. In the present paper the same technique is applied to study the local structure and dynamics of NH_4^+ ions in a rigid dehydrated zeolite-A. During the preliminary equilibration, the unstable $NH_4(4)$ type ion (the 12th ion) is pushed down to near a more stable 6-ring position in the α-cage that is already associated with an $NH_4(1)$ type ion (the 1st) in the β-cage, which moves to another 6-ring position in the β-cage that is already associated with an $NH_4(2)$ type ion (the 7th) in the α-cage. Calculated x, y, and z coordinates of some NH_4^+ ions are in good agreement with those obtained from an X-ray diffraction experiment except that no $NH_4(4)$ type ion is found and there are six $NH_4(2)$ type ions instead of 0.5 and 5.5 occupancy. The analyses of calculated interatomic distances and time correlation functions of these ions indicate that the $NH_4(1-1)$ and $NH_4(3)$ type ions are associated loosely with only one O(3) atom of the 6-ring and with only one O(1) atom of the 8-ring windows, respectively, while the $NH_4(1-2)$ and $NH_4(2)$ type ions are associated strongly with two or three O(3) atoms of the 6-ring windows in the α- and β-cages, respectively. The analysis of hydrogen bond time correlation functions of these ions indicate that about one, two or three, three, and one hydrogen bond of each $NH_4(1-1)$, $NH_4(1-2)$, $NH_4(2)$ and $NH_4(3)$ type ion is kept for 1.4, 21, 75, and 1.4 ps, respectively, before breakup of the hydrogen bond occurs and significant exchange of O atom hydrogen-bonded to the ion.

KEY WORDS: Zeolite-A, dynamics, ion positions.

1 INTRODUCTION

In previous studies, we have performed molecular dynamics (MD) simulations of three different zeolite-A systems: a rigid dehydrated zeolite-A [1], two rigid Ca^{2+}-exchanged zeolite-A [2], and a rigid hydrated zeolite-A [3]. In the first paper [1], a best-fitted set of electrostatic charges was chosen from the results of the MD simulation at 298.15 K and Ewald summation [4] was used for the long-ranged character of Coulomb interaction. The calculated x, y, and z coordinates of Na^+ ions were in good agreement with the positions determined by an X-ray crystallography [5] within statistical errors. Their random motions in different types of closed cages were well described by time-correlation functions and Na_I type ions were found to be less diffusive than Na_{II} and Na_{III}. At 600.0 K, the unstable Na_{III} type ion pushes one of the nearest Na_I ions into the β-cage and sitted on the stable site I instead and the captured ion in the β-cage wandered over and attacked one of the eight Na_I ions.

In the second paper [2], the same method was applied to study the local structure and dynamics of cations in rigid dehydrated Ca^{2+}-exchanged zeolite-A systems, Ca_6-A and Ca_4Na_4-A. At 298.15 K, the calculated positions of Ca^{2+} and Na^+ ions were in poor agreement with those determined by X-ray diffraction experiments [6–7], but this was reasonably explained by large repulsive interactions between cations. A simple harmonic oscillation of Ca^{2+} ions in the dehydrated Ca_6-A zeolite and simultaneous random motions for the same kinds of cations in the dehydrated Ca_4Na_4-A zeolite due to a positional symmetry were observed in their velocity auto-correlation functions and mean square displacements. MD simulation of the fictitious Ca_8-A zeolite with $Ca^{1.5+}$ confirmed our results for the behavior of Ca^{2+} ions in the dehydrated Ca_6-A zeolite.

In the third paper [3], a rigid hydrated zeolite-A at 298.15 K was studied by MD simulation to investigate the local structure and dynamics of Na^+ ions and water molecules. The results of the MD simulation showed that eight Na_I type ions were kept at their sites of 6-ring windows, characterized by non-diffusive vibrational motion, and that four Na_{IV} type ions showed a diffusive mobility due to loose bindings to nearest framework atoms and full hydrations with α-cage water molecules. β-cage water molecules formed a distorted tetrahedron with edge lengths in good agreement with those predicted in an X-ray diffraction experiment [8]. However, there was no clear evidence for the dodecahedral arrangement of 20 water molecules predicted in an the X-ray diffraction experiment [8]. The dynamical behavior of α- and β-cage water was more diffusive than bulk water due to the lack of hydrogen bonds in the closed cages. The rotational motions of water molecules in both α- and β-cages were characterized by slower librational motions and faster rotational relaxations than bulk water. An MD simulation in the true cell showed very little sensitivity of the structure and dynamics of Na^+ ions and water molecules to the size of the zeolite framework.

As McCusker and Seff pointed out [9], the zeolite-A framework can accommodate 11 cations relatively well at the eight 6-ring and three 8-ring sites in each pseudocell, but that is one short of the 12 sites needed by monopositive cations to balance the 12-anionic charges. Consequently, the twelfth ion must occupy a somewhat less satisfactory position in the structure. In the dehydrated zeolite-A system, this cation position is located in the large cavity opposite to a 4-ring [2]. A similar position is observed for a Tl^+ ion in Cs_9Tl_3-A zeolite system [10]. From the view of our MD simulation result [1], the second possible site for the twelfth ion is inside the β-cage as observed in the MD simulation study of the dehydrated zeolite-A at 600.0 K–eight Na_I type ions at the eight 6-ring sites, three Na_{II} type at the three 8-ring, and one inside the β-cage. But there was a different MD result for the same system at 600.0 K by Shin *et al.* [11], in which the Na_{III} ion, initially located at the large cavity opposite to a 4-ring (site III), attacks one of the three neighboring 8-ring sites (site II). At the same time, the attacked Na_{II} type ion moves to one of another neighboring sites III with Na_I type ions remaining near the 6-ring sites (Site I). They called this "concerted transport process" [11].

Since, in a NH_4^+-exchanged zeolite-A system, the size of NH_4^+ ion is larger than that of Na^+ ion so that the NH_4^+ ion must associate with O atoms of the zeolite-A framework via hydrogen bonds, it may be less adaptable than either Na^+ or Tl^+ and therefore may select a different twelth-cation site. The result of X-ray diffraction experiment [9] for this zeolite-A system showed that 0.5 of this ion sits on a 6-ring that is already associated with another NH_4^+ ion and 0.5 sits on the large cavity opposite to a 4-ring.

Continuing the MD simulations of three different zeolite-A systems, we have chosen the rigid NH_4^+-exchanged zeolite-A as the fourth object in the series of our studies on the zeolite-A system. The primary purpose of this work is to investigate the local structure and dynamics of NH_4^+ ions in the rigid NH_4^+-exchanged zeolite-A using the previously determined potential parameters and the Ewald summation technique [4] with the determination of the Lennard-Jones parameters for the NH_4^+ion.

In Section II we present the molecular models and MD simulation method. We discuss our simulation results in Section III and present the concluding remarks in Section IV.

2 MOLECULAR MODELS AND MD SIMULATION

The NH_4^+-exchanged zeolite-A framework is modeled by the pseudocell, $(SiAlO_4)_{12}$, of the Pm3m space group ($a = 12.284$ Å) which contains 12 NH_4^+ ions. The framework is assumed to be rigid and the framework atoms are fixed in the space at the positions determined by the X-ray diffraction experiment of McCusker and Seff [9]. Table 1 shows the idealized occupancy of N atoms of NH_4^+ ions which is obtained from the experiment. 8.5 NH_4^+ions per pseudo-cell are associated with 6-ring positions of the zeolite-A framework: 3.0 recessed 1.80 Å into the sodalite cavity (the $NH_4(1)$ type) and 5.5 extending 1.43 Å into the large cavity (the $NH_4(2)$ type), 3.0 are associated with 8-ring positions (the $NH_4(3)$ type), and 0.5 opposite to a 4-ring (the $NH_4(4)$ type). The fractional occupancy observed at the $NH_4(2)$ and $NH_4(4)$ type ions indicates the existence of 2 types of pseudo-cells in the unit cell. Four pseudo-cells have 3 $NH_4(1)$, 5 $NH_4(2)$, 3 $NH_4(3)$, and 1 $NH_4(4)$ type ions (the 1st pseudo-cell) and the remainder four have 3, 6, 3, and 0 (the 2nd pseudo-cell).

Table 1 Idealized occupancy of NH_4^+ ions in the NH_4^+ -exchanged zeolite-A.[a]

type of NH_4^+ ion	*Fm3c*[b]	*Pm3m*[c]	*this work*
$NH_4(1)$: near 6-ring, recessed 1.80 A into β-cage	24.0 (25.8)	3.0 (3.2)	3.0
$NH_4(2)$: near 6-ring, extended 1.43 A into α-cage	44.0 (43.6)	5.5 (5.5)	5.0
$NH_4(3)$: near 8-ring	24.0 (21.6)	3.0 (2.7)	3.0
$NH_4(4)$: opposite of 4-ring	4.0 (4.0)	0.5 (0.5)	1.0

[a]The numbers in ( ) are refined occupancy factors. [b]Unit cell. [c]Pseudo-cell.

Based on this occupancy, the positions of the N atoms of NH_4^+ ions (1st pseudo-cell) are listed in Table 2. The distances between N atoms in NH_4^+ ions for this configuration are calculated and listed in Table 3. The shortest distance of 2.973 Å comes from between 6th and 12th ions in Table 2 and 3.22 Å from between two ions which confront each other through a 6-ring window (2nd pseudo-cell). The configuration of Table 2 is the most probable one because the distances between N atoms in NH_4^+ ions are distributed as far as possible. However, there may be another configuration, which is the same as a stereoview of a likely atomic arrangement pointed out in the paper of Karl Seff and co-worker [9] but is relatively improbable because of the short distance (2.619 Å) between N(1) atoms. In both configurations, the occupancy factors of the $NH_4(1)$, $NH_4(2)$, $NH_4(3)$ and $NH_4(4)$ type ions are respectively 3.0, 5.0, 3.0 and 1.0 (Table 1). Our MD simulation is initialized with the positions of N atoms in NH_4^+ ions for the configuration listed in Table 2 and with those of H atoms determined randomly, after the determination of the LJ parameter, σ, for NH_4^+ ion by comparing MD calculated positions of N atoms of NH_4^+ ions for several σ's simulated from these positions of N and H atoms.

The interaction potential for cations and framework atoms is given as a sum of Lennard-Jonnes (LJ) and Coulomb potentials between each NH_4^+ ion i and each

Table 2 Initial positions (Å) of N atoms of NH_4^+ ions.

type	*ion*	*position*		
		x	y	z
$NH_4(1)$	1	4.833	4.833	4.833
	2	4.833	−4.833	−4.833
	3	−4.833	−4.833	4.833
$NH_4(2)$	4	−2.973	2.973	2.973
	5	2.973	−2.973	2.973
	6	2.973	2.973	−2.973
	7	−2.973	2.973	−2.973
	8	−2.973	−2.973	−2.973
$NH_4(3)$	9	5.707	0.423	0.423
	10	0.423	5.707	0.423
	11	0.423	0.423	5.707
$NH_4(4)$	12	2.960	2.960	0.000

Table 3 Initial distances (Å) between N atoms of NH_4^+ ions.

type-type	*exp.**	*Table 2*
N(1)—N(1)	3.70	3.704
N(1)—N(2)	3.22	5.193
N(2)—N(4)	–	2.973
N(3)—N(4)	–	3.763

*Reference 9.

framework atom j as follows:

$$\Phi = \sum_{i<j}^{\text{ion}} \sum \phi_{ij} + \sum_{i}^{\text{ion}} \sum_{j}^{\text{frame}} \varphi_{ij} \tag{1}$$

where the interaction energies ϕ_{ij} and φ_{ij} are expressed as

$$\phi_{ij} = 4\varepsilon\left(\frac{\sigma^{12}}{r^{12}} - \frac{\sigma^{6}}{r^{6}}\right) + \sum_{k}^{i} \sum_{l}^{j} \frac{q_k q_l}{r_{kl}} \tag{2}$$

and

$$\varphi_{ij} = 4\varepsilon\left(\frac{\sigma^{12}}{r^{12}} - \frac{\sigma^{6}}{r^{6}}\right) + \sum_{k}^{i} \frac{q_k q_j}{r_{kj}} \tag{3}$$

with $r = r_{ij}$, and k and l represent the atoms of NH_4^+ ion. The LJ parameters and electrostatic charges of framework atoms were determined in a previous work [1] by comparing the interatomic distances of the dehydrated zeolite-A system.

For the NH_4^+ ion, a rigid Bernal-Fowler-like model for liquid ammonia [12] is modified and used. The bond length N-H and the bond angle ∠HNH are fixed at 1.0126 Å and 109.5° so that the H-H distance is fixed at 1.6536 Å. The total electrostatic charge on NH_4^+ ion should be given as 0.55 e like Na^+ ion according to the previous work [1] and distributed -0.1447 e on N atom and 0.1737 e on each H atom. These partial charges of N and H atoms are determined by using Huheey's electronegativity set [13], Sanderson's electronegativity equalization principle [14], and the electric neutrality principle. For the liquid ammonia case [12], 0.485 e on each H atom plus a neutralizing charge -1.455 e on the molecular C_{3v} axis 0.156 Å from the N atom, inside the molecule. The LJ parameter, ε, of NH_4^+ ion is chosen to be equal to that of NH_3 which was used in Ref. 12, but the other LJ parameter, σ, is optimized by comparing the agreement between the crystallographic positions [9] and our MD calculated positions of 11 N atoms of NH_4^+ ions at the various values of σ as shown in Table 4.

Table 4 Absolute values of the differences between crystallographic and calculated positions of 11 NH_4^+ ions at various values of Lennard-Jones parameter, σ (Å).

type of ion		$\sigma = 3.00$	3.10	3.20	3.30	3.40
$NH_4(1)$	ΔX_1	0.385	0.338	0.332	0.334	0.299
	ΔY_1	0.310	0.252	0.220	0.190	0.152
	ΔZ_1	0.388	0.340	0.333	0.328	0.304
$NH_4(2)$	ΔX_2	0.076	0.031	0.009	0.057	0.104
	ΔY_2	0.092	0.045	0.021	0.038	0.082
	ΔZ_2	0.076	0.029	0.009	0.058	0.104
$NH_4(3)$	ΔX_3	0.342	0.345	0.352	0.361	0.362
	ΔY_3	0.053	0.021	0.025	0.056	0.090
	ΔZ_3	0.347	0.344	0.357	0.358	0.360
total	ΔT^*	6.695	5.445	5.052	5.646	6.151

$^*\Delta T = 3\Delta X_1 + 3\Delta Y_1 + 3\Delta Z_1 + 5\Delta X_2 + 5\Delta Y_2 + 5\Delta Z_2 + 3\Delta X_3 + 3\Delta Y_3 + 3\Delta Z_3$.

The choice of 0.55 e for the total charge on NH_4^+ is enforced by the previous works [1–3]. Several values of q_{Na^+} (0.55, 0.6, 0.625, 0.65, and 0.7 e) have been carefully examined by calculating the average distances of Na^+ ions from the center of the α-cage and the interatomic distances between Na^+ ions and between Na^+ ion and O atoms of the framework in the rigid zeolite-A system [1]. The result of $q_{Na^+} = 0.55$ e has been selected as the best one, in view of the accuracy in the distance of the Na_{III} type ion from the center of the α-cage and the interatomic distance of Na-O. No *et al.* [15] have obtained the potential energy functions of dehydrated zeolite-A by constrained method, using the geometry of $(T_2O_4Na)_n$ from an X-ray crystallographic study [16]. Force constant sets are calculated with these potential functions at several q_{Na^+} values (0.1, 0.25, 0.40, 0.55, 0.71, and 1.0 e). With the force constant sets, normal-mode calculation is performed, and the result is compared with the far-IR spectra[17–19] of the hydrated zeolite-A. The average net charge of Na^+ is 0.625 e. These potential energy parameters have been used for MD simulation of the rigid dehydrated zeolite-A system [11]. The use of 0.65 e for the charge of Na^+ in nonbonded sodium-sodium has been reported in MD simulation of zeolite NaY [20]. However, the electrostatic potential of the zeolite framework was modeled by partial atomic charges of 1.0 e on the sodium atoms and −0.125 e on the O atoms [20].

The LJ parameters and electrostatic charges used in this work are shown in Table 5. The potential parameters used for the zeolite-A framework atoms are already obtained in our previous study [1]. The long-ranged Coulomb potential between the electrostatic charges on the cations and framework atoms is treated with the Ewald summation, which was discussed in detail in Section II of Refs. 1 and 3.

A canonical ensemble of fixed N (number of particles), V (volume of zeolite), and T (temperature) is chosen for the MD simulation ensemble. Gauss's principle of least constraint [21] is used to maintain the system at a constant temperature. The ordinary periodic boundary condition in the x-, y-, and z-direction and minimum image convention are applied for the Lennard-Jones potential with a spherical cut-off of radius 6.142 Å. Gear's fifth order predictor-corrector method [22] is used to solve the equations of translational and rotational motions numerically with time step of 1.00×10^{-15} sec. For the internal orientation of the rigid geometry of NH_4^+ ion, Evans's quaternion method [23] is used [3,24]. The equilibrium properties are

Table 5 Lennard-Jones parameters and electrostatic charges used in this work.

ions and atoms	*σ(Å)*	*ε(kJ/mol)*	*charge(e)*
NH_4^+ ion	3.200	1.164	(0.55)
N atom	–	–	−0.1447
H atom	–	–	0.1737
Al(=Si) atom	4.009	0.5336	0.6081
O(1) atom	2.890	0.6487	−0.4431
O(2) atom	2.890	0.6487	−0.4473
O(3) atom	2.890	0.6487	−0.4380

averaged over four blocks of 100,000 time steps (100 ps), for a total of 400,000 time steps after 100,000 time steps to reach equilibrium. The configurations of NH_4^+ ions are stored every 5 time steps for further analysis.

3 RESULTS AND DISCUSSION

We begin by reporting the inital behavior of NH_4^+ ions in the preliminary simulation run for equilibration. During the equilibration run of 100,000 time steps (100 ps), some of NH_4^+ ions move and finally arrive at their stable sites within about 50,000 time steps where they remain with non-diffusive vibrational motion till the end of the whole simulation. Figure 1 shows the stereoplots, by ORTEP [25], of (a) 12 NH_4^+ ions viewed from the α-cage and (b) 8 NH_4^+ ions from the β-cage of a rigid dehydrated zeolite-A at 298.15 K after 500,000 time steps (the y and z of the box run from + to − in Figure 1(a)). All the movement of NH_4^+ ions is initially due to the unstable $NH_4(4)$ type ion (the 12th ion): this ion is only 2.973 Å away from an $NH_4(2)$ type ion (the 6th ion) as shown in Table 2 and 3, and the repulsive interaction between these two ions pushes the $NH_4(4)$ type ion to near a more stable 6-ring position that is already associated with an $NH_4(1)$ type ion (the 1st ion) in the

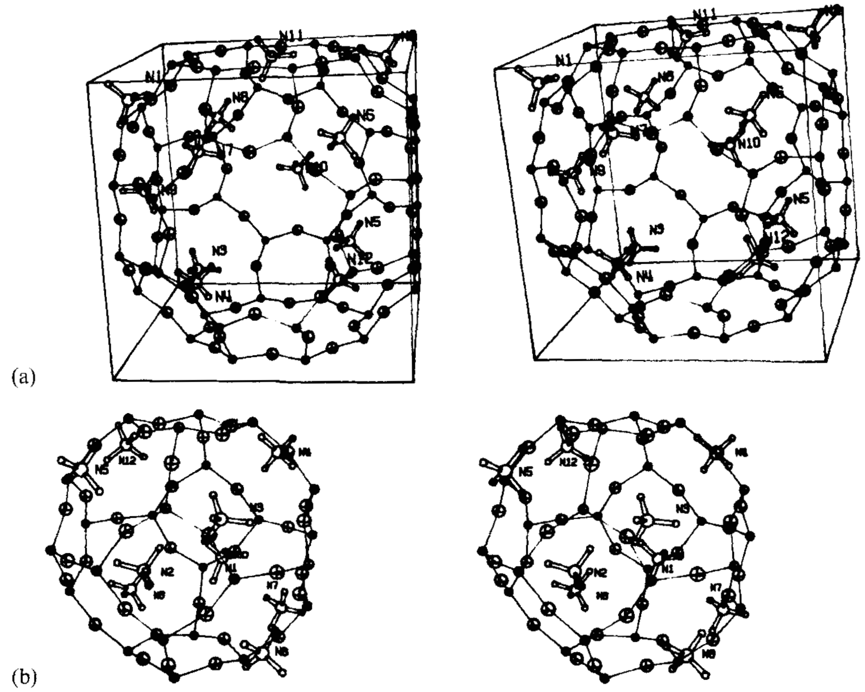

Figure 1 Stereoplots of (a) 12 NH_4^+ ions viewed from the α-cage and (b) 8 NH_4^+ ions from the β-cage of a rigid dehydrated zeoilte-A at 298.15 K after 500,000 time steps (the y and z run from + to − in Figure (a)).

sodalite cavity (β-cage). This situation is exactly the same as that of our previous MD simulation on a rigid dehydrated zeolite-A system at 600 K [1] – the unstable Na_{III} type ion pushed down one of the nearest Na_I ions into the β-cage and sits on the stable site I instead and the captured ion in the β-cage wandered over and attacked one of the eight Na_I ions. The effect of high temperature causes the same structural change in a rigid zeolite-A system as that of large ion size – a loosely bounded ion is wandering over the sodalite cavity. It is worth noting that the same movement of the 12th ion is always observed in the MD simulations at the various values of σ to determine the σ of N atom of NH_4^+ ion.

The 12th ion migrates to the stable 6-ring position and becomes the $NH_4(2)$ type ion. The behavior of the 1st ion is very interesting! Initially this ion is sitted on one (+, +, +) of the stable 6-ring positions in the sodalite cavity as shown in Table 2, but upon the attack of the migrated 12th ion, it may stay there to confront the 12th ion or move to one of the other stable 6-ring positions (−, +, +; +, −, +; +, +, −; −, +, −; −, −, −) in the sodalite cavity to confront one of the five $NH_4(2)$ type ions. In the case of movement, however, there is only one choice – it takes the (−, +, −) 6-ring position in the sodalite cavity to confront the 7th ion as shown in Figure 1 since then it is away from the other two $NH_4(1)$ type ions (the 2nd and 3rd) as far as possible. For the configuration after the migration of the 12th ion to the (+, +, +) 6-ring position in the large cavity (α-cage), both sites of the 1st ion, the (+, +, +) and the (−, +, −) 6-ring positions in the sodalite cavity that confront the 12th ion and the 7th ion, respectively, are exactly identical with respect to the positions of the five $NH_4(2)$ and the two $NH_4(1)$ type ions, but not those of the three $NH_4(3)$ type ions.

Averaged x, y, and z coordinates of N atoms of NH_4^+ ions and their distances, r, from the center of box at 298.15 K for the sampling run of 400,000 time steps (400 ps) are listed in Table 6. The predicted sites of some NH_4^+ ions by our MD simulation are in good agreement with those obtained from the X-ray diffraction experiment [9]. However, Table 6 shows that no $NH_4(4)$ type ion is found and there

Table 6 Average x, y, and z coordinates (Å) of N atoms of NH_4^+ ions and distances, r(A), from the center of box at 298.15 K for 400,000 time steps (400 ps).

type	*ion*	*x*	*y*	*z*	*r*
$NH_4(1)$	1	-5.430 ± 0.164	4.591 ± 0.076	-5.435 ± 0.166	8.952 ± 0.160
	2	4.632 ± 0.019	-4.624 ± 0.014	-4.638 ± 0.018	8.022 ± 0.025
	3	-4.635 ± 0.020	-4.623 ± 0.018	4.631 ± 0.016	8.019 ± 0.026
$NH_4(2)$	4	-2.986 ± 0.026	2.968 ± 0.029	2.986 ± 0.026	5.161 ± 0.046
	5	2.969 ± 0.028	-3.011 ± 0.020	2.965 ± 0.032	5.164 ± 0.045
	6	2.981 ± 0.028	2.971 ± 0.030	-2.985 ± 0.027	5.160 ± 0.048
	7	-2.979 ± 0.035	2.999 ± 0.029	-2.974 ± 0.035	5.168 ± 0.056
	8	-2.961 ± 0.029	-3.005 ± 0.022	-2.961 ± 0.030	5.154 ± 0.046
	12	2.981 ± 0.030	3.001 ± 0.026	2.983 ± 0.029	5.176 ± 0.048
$NH_4(3)$	9	-5.941 ± 0.047	-0.392 ± 0.026	0.000 ± 0.043	5.954 ± 0.037
	10	0.012 ± 0.038	-5.700 ± 0.012	0.005 ± 0.046	5.700 ± 0.012
	11	0.012 ± 0.030	-0.387 ± 0.030	-5.937 ± 0.029	5.950 ± 0.029

are six $NH_4(2)$ type ions instead of 0.5 and 5.5 occupancy as shown in Table 1. The average positions of the 1st ion and three $NH_4(3)$ type ions (the 9th, 10th, and 11th) are moved a lot from the initial positions given in Table 2, in addition to the movement of the 12th ion which is the major cause for all the movement. The unsymmetry of x, y, and z coordinates of the 1st ion seems caused by the interaction with the two $NH_4(1)$ type ions in the sodalite cavity and causes the unsymmetry of positions of the three $NH_4(3)$ type ions. This unsymmetry affects the interatomic distances shown in Tables 8 and 9.

Averaged potential energies of NH_4^+ ions at 298.15 K for the 400,000 time steps (400 ps) are listed in Table 7. The order of stability of these ions is the $NH_4(3)$, the $NH_4(2)$, and the $NH_4(1)$ type, in comparison with the dehydrated zeolite-A system [1], – the Na_I (6-ring), the Na_{II} (8-ring), and the Na_{III} type (opposite to a 4-ring). The highest energy of the 1st ion and a higher energy of the 7th ion than that of the other usual $NH_4(2)$ type ions (the 4th, 6th, and 12th) is attributed to the fact that the two ions are associated with the same 6-ring and confront each other through the 6-ring window. However, the large difference in the amount of the potential energies of these ions indicate that the 7th ion is strongly associated with the 6-ring window while the 1st ion is weakly associated since the former was already associated with it

Table 7 Average potential energy(kJ/mol) of each NH_4^+ ion at 298.15 K for 400,000 time steps (400 ps).

type	*ion*	*Energy*	*⟨Energy⟩*
$NH_4(1)$	1	-46.3 ± 1.5	-69.0 ± 16.1
	2	-80.4 ± 3.2	
	3	-80.3 ± 2.8	
$NH_4(2)$	4	-92.0 ± 6.1	-90.0 ± 1.5
	5	-88.6 ± 6.1	
	6	-91.8 ± 6.4	
	7	-89.2 ± 7.1	
	8	-88.3 ± 5.6	
	12	-90.1 ± 6.5	
$NH_4(3)$	9	-92.5 ± 1.9	-92.5 ± 0.0
	10	-92.5 ± 2.0	
	11	-92.5 ± 2.0	

Table 8 Calculated interatomic distances (Å)between N atoms of NH_4^+ ions from Table 6.*

type-type	*distances*
$NH_4(1)$—$NH_4(1)$	3.87 (1–2, 3), 4.27 (2–3)
$NH_4(1)$—$NH_4(2)$	4.86 (1–4, 6), 3.82 (1–7), 5.23 (2–5, 6, 8 & 3–4, 5, 8)
$NH_4(2)$—$NH_4(3)$	5.04 (5, 8–9, 10, 11), 5.52 (4, 6, 7, 12–9, 10, 11)

* the numbers in ( ) are those between ions.

Table 9 Calculated distances (Å) of N atoms of NH_4^+ ions from the center of box (CB) and interatomic distances between N atoms of NH_4^+ ions and 0 atoms of the zeolite-A framework from Table 6.

distances	*exp.*[a]	*this work*
CB-NH_4(1)	8.371	8.33 (1, 2, 3)
CB-NH_4(2)	5.149	5.16 (4, 5, 6, 7, 8, 12)
CB-NH_4(3)	5.738	5.87 (9, 10, 11)
CB-NH_4(4)	4.186	–
NH_4(1)—O(2)	3.46	3.51 (1)[b], 3.28 (2, 3)[c]
NH_4(1)—O(3)	2.99	2.91 (1)[b], 2.80 (2, 3)[c]
NH_4(2)—O(2)	3.221	3.21 (4, 5, 6, 7, 8, 12)[d]
NH_4(2)—O(3)	2.789	2.78 (4, 5, 6, 7, 8, 12)[d]
NH_4(3)—O(1)	2.94	3.32 (10)[b], 2.92 (9, 11)[e]
NH_4(3)—O(2)	3.07	3.65 (10)[b], 3.38 (9, 11)[e]
NH_4(4)—O(1)	3.20	–
NH_4(4)—O(2)	3.07	–
NH_4(4)—O(3)	2.789	–

[a] Reference 9. [b] Only one value. [c] Average of 6 values. [d] Average of 18 values. [e] Average of 2 values.

in the α-cage when the latter is pushed down to the 6-ring in the β-cage due to the attack of the 12th ion. The highest potential energy of the 1st ion also seems related to the short distances (3.87 Å) to the two NH_4(1) type ions which also have higher energies than those of the NH_4(2) type ions. The relatively higher energies of the 5th and 8th ions than that of the other NH_4(2) type ions (the 4th, 6th, and 12th) are also notable. This seems related to the interatomic distances shown in Tables 8 and 9.

Averaged interatomic distances between N atoms of NH_4^+ ions and between N atoms of NH_4^+ ions and O atoms of the zeolite-A framework calculated from the positions of N atoms of NH_4^+ ions in Table 6 are listed in Tables 8 and 9. The shortest distance between N atoms of NH_4^+ ions is NH_4(1)–NH_4(2) (1 – 7), which means that the 1st and 7th ions are associated with the same 6-ring and confront each other through the 6-ring window. The difference between the same NH_4(1)–NH_4(1) distances which are 3.87Å (1 – 2, 3) and 4.27Å (2 – 3) is noticeable. This can be easily understood when one looks at the NH_4(1) – O(2) and NH_4(1) – O(3) distances in Table 9 – the 2nd and 3rd ions can make strong associations with three O(3) atoms at each 6-ring position in the sodalite cavity while the 1st ion is only loosely bound to only one O(3) atom apparently because of the 7th ion confronting it. This behavior of 1st ion is also seen in time dependent autocorrelation functions, specially in the mean square displacement of the ion. Among the NH_4(1) – NH_4(2) distances in Table 8, the 4th and 6th ions are near the 1st ion while the 5th, 6th, and 8th are near the 2nd and the 4th, 5th, and 8th near the 3rd: both the 5th and 8th are near the 2nd and 3rd. The shorter NH_4(2)–NH_4(3) distance than the other is due to the 5th and 8th ions. This seems related to the somewhat higher energies of those ions.

Calculated distances of N atoms of the NH_4 type ions from the center of box give an overall agreement with those obtained from the X-ray diffraction experiment[9]

Table 10 Calculated distances (Å) between H atoms of NH_4^+ ions and O atoms of the zeolite-A framework for the final positions after the whole 500,000 time steps.

NH_4^+ ion		*Framework*		*Distance*	*NH_4^+ ion*		*Framework*		*Distance*
No.	*H atom*	*No.*	*O atom*		*No.*	*H atom*	*No.*	*O atom*	
1	H(3)	62	O(3)	2.335	7	H(1)	38	O(3)	2.444
	H(4)	38	O(3)	1.842		H(2)	62	O(3)	1.977
						H(3)	17	O(3)	2.189
2	H(2)	35	O(3)	1.979	8	H(1)	32	O(3)	1.823
	H(4)	50	O(3)	2.183		H(3)	14	O(3)	1.685
	H(4)	51	O(2)	2.372		H(4)	68	O(3)	1.806
3	H(1)	71	O(3)	1.911	12	H(1)	59	O(3)	1.917
	H(2)	26	O(3)	1.726		H(2)	47	O(3)	1.785
	H(3)	20	O(3)	2.269		H(4)	5	O(3)	1.742
4	H(1)	23	O(3)	1.852	9	H(1)	30	O(1)	1.706
	H(2)	63	O(2)	2.589		H(3)	36	O(1)	2.422
	H(3)	44	O(3)	1.786					
5	H(1)	29	O(3)	2.034	10	H(2)	6	O(1)	2.454
	H(3)	2	O(3)	2.088		H(3)	24	O(1)	2.420
	H(4)	53	O(3)	1.681					
6	H(1)	41	O(3)	1.688	11	H(1)	54	O(1)	2.206
	H(2)	11	O(3)	1.858		H(4)	72	O(1)	2.353
	H(3)	56	O(3)	1.501					

as shown in Table 9, even though no $NH_4(4)$ type ion is predicted in our MD simulation. All the six $NH_4(2)$ type ions have strong associations with three O(3) atoms at each 6-ring position in the large cavity. This behavior is also seen in the cosine auto-correlation functions of these ions. The longer $NH_4(3) - O$ distances of the 10th ion than those of the others (the 9th and 11th) indicate a weaker association with the O(1) atom at the 8-ring position which seems related to the unsymmetry of position of the 10th ion, when compared with those of the other $NH_4(3)$ type ions (the 9th and 11th). The unsymmetry of the calculated x, y, and z coordinates of the 1st (compared with the 2nd and 3rd) and the 10th (compared with the 9th and 11th) shown as in Table 6 remains unexplained except to indicate rearranged, stable positions of the NH_4^+ ions by the force field of the ions and framework atoms of the zeolite-A framework from the disturbance which is caused by breakup of the positional symmetry due to the movement of the $NH_4(4)$ type ion (the 12th).

Distances of hydrogen bonds between H atoms of NH_4^+ ions and O atoms of zeolite-A framework for the final configuration after the whole 500,000 time steps are listed in Table 10. This configuration is also used to draw the streoplots in Figure 1. Since NH_4^+ ions are vibrating at their stable sites and rotating continually, the average value of hydrogen bond length of each NH_4^+ ion cannot be obtained so that the result in Table 10 gives hydrogen bond lengths only for an instant. One can see that some hydrogen bonds are loosely associated and that the number of the hydrogen bonds per an ion is about 1 – 2 for the $NH_4(1)$ and $NH_4(3)$ type ions and 3 for the $NH_4(2)$ type ions for the instant, if each distance between H atom of NH_4^+ ions and O atom of zeolite-A framework amounting to less than or equal to 2.1 Å is counted as a hydrogen bond. The $NH_4(1)$ and $NH_4(2)$ type ions hydrogen bond mostly to O(3) atoms of zeolite-A framework while the $NH_4(3)$ type ions are H-bonded mostly to O(1). The two NH_4^+ ions (the 1st and 7th) associating with the same 6-ring form hydrogen bonds to the same O(3) atoms (the 38th and 62th atoms of zeolite-A framework); a bond associated with an ion is short and the other is long, and vice versa. Time dependent behavior of the hydrogen bonds of each NH_4 type ion is discussed below.

Now we turn our attention to the dynamics of NH_4^+ ions. As discussed above, some ions are moving a lot but the others not. The NH_4^+ ions are classified according to the three types of them – the $NH_4(1)$, $NH_4(2)$, and $NH_4(3)$ type. But among the $NH_4(1)$ type ions, the dynamic behavior of the 1st ion is different from those of the others (the 2nd and 3rd) so that the dynamic properties of these ions are further classified into the $NH_4(1-1)$ type for the 1st ion, the $NH_4(1-2)$ type for the 2nd and 3rd ions, the six $NH_4(2)$ type ions, and the three $NH_4(3)$ type ions. Averaged, normalized velocity auto-correlation (VAC) functions and mean square displacements (MSD) of these four types of NH_4^+ ions are plotted in Figures 2 and 3. The VAC functions of the $NH_4(1-2)$ and $NH_4(2)$ type ions are very similar and those of the $NH_4(1-1)$ and $NH_4(3)$ type are also similar but not that much. The MSD's of these ions agree with this behavior. The $NH_4(1-1)$ type ion does a loose association with only one O(3) atom of the 6-ring window in the β-cage so that it diffuses into the β-cage with the change of O(3) atom associated with it. Each of the $NH_4(3)$ type ions is also associated with only one O(1) atom of the 8-ring window but it

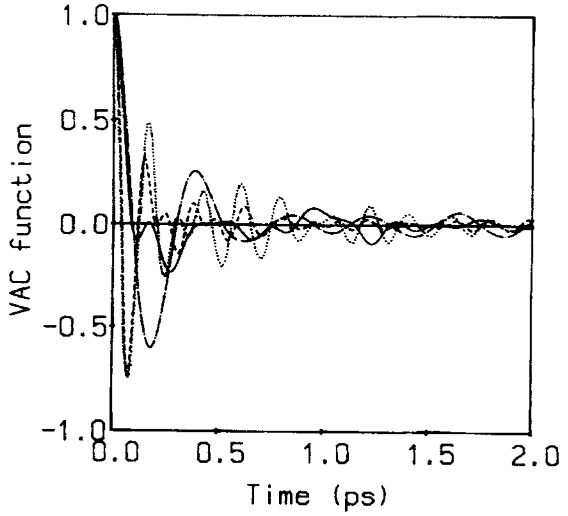

Figure 2 Normalized velocity auto-correlation functions of four types of NH_4^+ ions at 298.15 K: —— $NH_4(1-1)$, - - - $NH_4(1-2)$, -·-·- $NH_4(2)$, and ...... $NH_4(3)$ type.

moves within the plane of each 8-ring window so that MSD's of these type ions are not so big as that of the $NH_4(1-1)$ type ion. The $NH_4(1-2)$ and $NH_4(2)$ type ions are strongly associated with three O(3) atoms of the 6-ring windows in the α- and β-cages, respectively, so that the MSD's of these types ions are small and almost time independent for the whole simulation time.

In Figures 4 and 5, angular velocity auto-correlation (AVAC) and cosine auto-correlation (CAC) functions of the NH_4^+ ions are plotted. The CAC function,

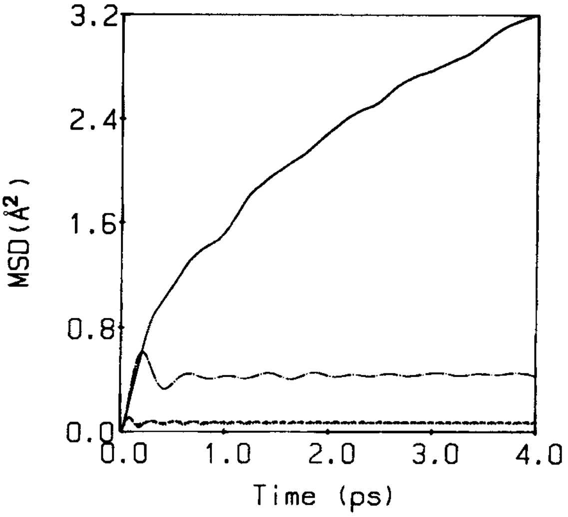

Figure 3 Mean square displacements of four types of $NH_4{}^+$ ions at 298.15 K. The notation is same as in Figure 2.

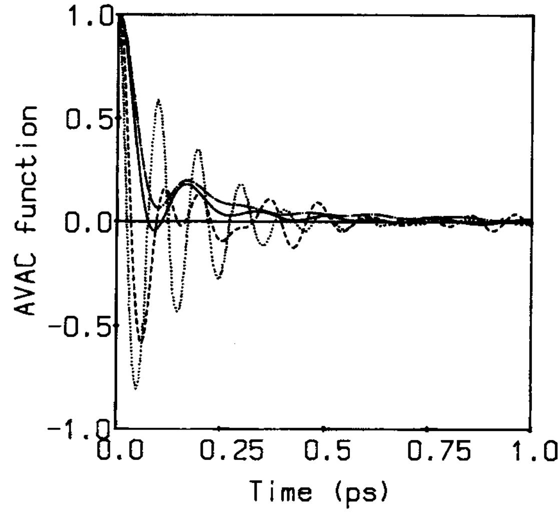

Figure 4 Normalized angular velocity auto-correlation functions of four types of $NH_4{}^+$ ions at 298.15 K. The notation is same as in Figure 2.

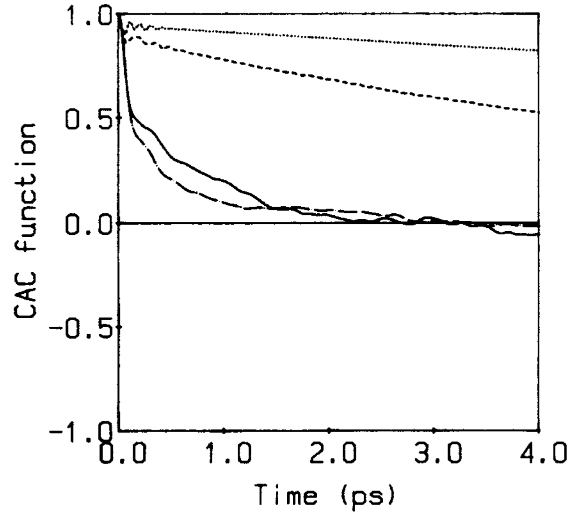

Figure 5 Normalized cosine auto-correlation functions of four types of NH_4^+ ions at 298.15 K. The notation is same as in Figure 2.

$\langle \cos\phi(t) \rangle$, of a rigid molecule is defined as $\langle \cos\phi(t) \rangle = \langle u_x(0)u_x(t) + u_y(0)u_y(t) + u_z(0)u_z(t) \rangle$ where $u_i(t)$ is the i component of the direction vector of molecular axis with unit magnitude at time t and $\phi(t)$ is the angle between the molecular axis and the z-axis at time t. Here one can find again the similarity of these functions between the $NH_4(1-1)$ and $NH_4(3)$ type ions and between the $NH_4(1-2)$ and $NH_4(2)$ type ions. The AVAC functions of the former suggest a slow change of angular velocities (big rotational motions) of them with slow vanishing tails of correlation (no recovery of the initial angular velocities) and the CAC functions of the $NH_4(1-1)$ and $NH_4(3)$ type ions show that these ions undergo a complete rotation due to a loose association with only one O(3) atom of the 6-ring and with only one O(1) atom of the 8-ring, respectively. On the other hand, the AVAC functions of the latter, especially the $NH_4(2)$ type ions, are rapidly oscillating with slowly decaying magnitudes which implies that these ions undergo much fast inversion of the rotational directions, but with very small change of the direction vectors as one can see the CAC functions of the $NH_4(1-2)$ and $NH_4(2)$ type ions due to strong associations with three O(3) atoms of the 6-ring windows in the α- and β-cages, respectively. The typical librational motion of water molecules in a hydrated zeolite-A and bulk system found in previous MD studies [3,26] has disappeared in this study since an NH_4^+ ion has the symmetry property of a spherical top.

In order to estimate the lifetime of hydrogen bonds between H atoms of NH_4^+ ions and O atoms of zeolite-A framework, we consider the hydrogen bond time

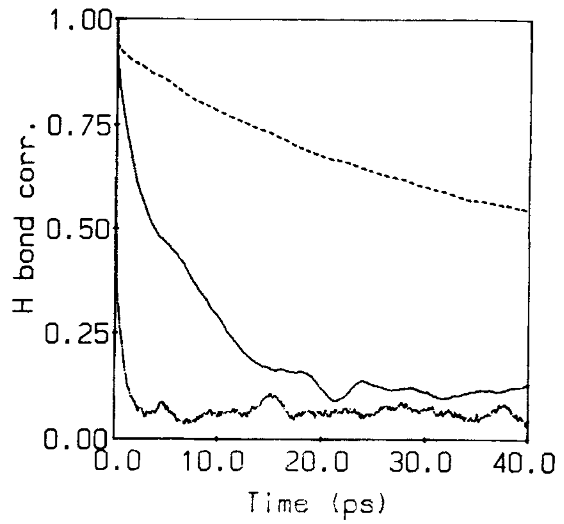

Figure 6 Normalized hydrogen bond time correlation functions of three different groups of $NH_4{}^+$ ions at 298.15 K: —— $NH_4(1-2)$ type, --- $NH_4(2)$ type, and ····· $NH_4(1-1)$ and $NH_4(3)$ type.

correlation function defined by

$$\langle R_i(t)\rangle = \left\langle \frac{\theta_i(0)\theta_i(t)}{\theta_i(0)\theta_i(0)} \right\rangle \tag{4}$$

where $\theta_i(t)$ is the Heaviside unit step function which is 1 if the distance between H atoms of NH_4^+ ions and O atoms of zeolite-A is less than or equal to 2.1 Å at time t and O otherwise (the subscript i indicates the i-th hydrogen bond).
The zero value of $\theta_i(0)$ is excluded in the average of $\langle R_i(t)\rangle$. The $\langle R_i(t)\rangle$ functions are determined by the strength of the hydrogen bonds and the stability of their sites. This time correlation function is somewhat similar to a residence time correlation function [27,28].

Figure 6 shows the time dependence of $\langle R_i(t)\rangle$ for the hydrogen bonds of three different groups of NH_4^+ ions (those for the $NH_4(1-1)$ and $NH_4(3)$ type ions are essentially the same). A characteristic decay time, τ, of the hydrogen bond is obtained by fitting the time correlation function to an exponential decay $\langle R_i(t)\rangle \approx \exp(-t/\tau)$ which is especially useful when τ is large. The results of our simulation indicate that about one, two or three, three, and one hydrogen bond of each $NH_4(1-1)$, $NH_4(1-2)$, and $NH_4(2)$ and $NH_4(3)$ type ion are kept for 1.4 (the fitting region: 0–3 ps), 21 (0–40), 75 (0–40), and 1.4 ps (0–3), respectively, before breakup of the hydrogen bond occurs and significant exchange of O atom hydrogen-bonded to the ion. The characteristic decay times of the hydrogen bond for these ions are in an agreed trend with the rotational relaxation times obtained by fitting the CAC functions of them to the same exponential decay, which are 0.57 (the fitting region: 0–2.7 ps), 7.5 (0–4), 28 (0–4) and 0.81 ps (0–3.3) for the $NH_4(1-1)$, $NH_4(1-2)$, $NH_4(2)$, and $NH_4(3)$ type ions, respectively.

4 CONCLUDING REMARKS

In the present paper, we have carried out a molecular dynamics (MD) simulation of NH_4^+ ions in a rigid dehydrated zeolite-A system at 298.15 K to elucidate the structure and dynamics of the NH_4^+ ions by using the previously determined Lennard-Jones parameters and electrostatic charges for the interactions between the NH_4^+ ions and framework atoms and the Ewald summation technique for the long-ranged character of Coulomb interaction.

Based on the results obtained from our MD simulation, the following conclusions may be drawn: During the preliminary equilibration, the unstable $NH_4(4)$ type ion (the 12th ion) is pushed down to near a more stable 6-ring position in the α-cage that is already associated with an $NH_4(1)$ type ion (the 1st) in the β-cage, which moves to another 6-ring position in the β-cage that is already associated with an $NH_4(2)$ type ion (the 7th) in the α-cage. The calculated x, y, and z coordinates of some NH_4^+ ions are in good agreement with those obtained from the X-ray diffraction experiment [9] except that no $NH_4(4)$ type ion is found and there are six $NH_4(2)$ type ions instead of 0.5 and 5.5 occupancy. The analyses of the calculated interatomic distances betweeen N atoms of NH_4^+ ions and O atoms of the zeolite-A framework, and the velocity auto-correlation(VAC) functions and mean square displacements (MSD) of these ions indicate that the $NH_4(1-1)$ and $NH_4(3)$ type ions are associated loosely with only one O(3) atoms of the 6-ring and with only one O(1) atom of the 8-ring windows, respectively, while the NH_4 $(1-2)$ and $NH_4(2)$ type ions are associated strongly with two or three O(3) atoms of the 6-ring windows in the α- and β-cages, respectively. The angular velocity (AVAC) and cosine autocorrelation (CAC) functions also show the similarity of the dynamic properties between $NH_4(1-1)$ and $NH_4(3)$ and between $NH_4(1-2)$ and $NH_4(2)$ type: the former undergoes a complete, big rotational motion without recovery of the initial angular velocity while the latter displays a fast inversion of the rotational direction with small change of the direction vector, which also indicates their association strength with O atom of the zeolite-A framework. The rotational relaxation times obtained by fitting the CAC functions of the NH_4^+ ions to an exponential decay are 0.57, 7.5, 28, and 0.81 ps for the $NH_4(1-1)$, $NH_4(1-2)$, $NH_4(2)$, and $NH_4(3)$ type ions, respectively. The analyses of the hydrogen bond time correlation functions of these ions indicate the same dynamic behavior: about one, two or three, three, and one hydrogen bond of each $NH_4(1-1)$, $NH_4(1-2)$, $NH_4(2)$, and $NH_4(3)$ type ion is kept for 1.4, 21, 75, and 1.4 ps, respectively, before breakup of the hydrogen bond occurs and significant exchange of O atom hydrogen-bonded to the ion.

The rigid framework approximation adopted for simplicity in the present work is physically less adequate in the study of cation exchanged zeolites. The inclusion of the intraframework interaction of zeolite-A is essential to take account of energy exchange between the adsorbed molecules and the framework atoms and dynamical couplings of the sorbate with framework vibrations, as well as the flexibility of the host lattice, and must be considered in the next study.

Acknowledgements

This work was supported by a research grant (KOSEF 901-0303-032-1) to SHL from the Korea Science and Engineering Foundation. The authors thank to the Computer Center at Korea Institute of Science and Technology for the access to the Cray-C90 system.

References

[1] G. K. Moon, S. G. Choi, H. S. Kim and S. H. Lee, "Molecular dynamics simulation studies of zeolite-A. I. Structure and dynamics of Na^+ ions in rigid dehydrated zeolite-A framework", *Bull. Kor. Chem. Soc.*, **13**, 317 (1992).

[2] G. K. Moon, S. G. Choi, H. S. Kim and S. H. Lee, "Molecular dynamics simulation studies of zeolite-A. II. Structure and dynamics of cations in rigid dehydrated Ca^{2+}-exchanged zeolite-A", *Bull. Kor. Chem. Soc.*, **14**, 356 (1993).

[3] S. H. Lee, G. K. Moon, S. G. Choi and H. S. Kim, "Molecular dynamics simulation studies of zeolite-A. 3. Structure and dynamics of Na^+ ions and water molecules in a rigid zeolite-A", *J. Phys. Chem.*, **94**, 1561 (1994).

[4] N. Anastasiou and D. Fincham, "Programs for the dynamic simulation of liquids and solids II. MDIONS: rigid ions using the Ewald sum", *Comput. Phys. Commun.*, **25**, 159 (1982).

[5] J. J. Pluth and J. V. Smith, "Accurate redetermination of crystal structure of dehydrated zeolite-A. Absence of near zero coordination of sodium. Refinement of Si, Al-ordered superstructure", *J. Am. Chem. Soc.*, **102**, 4704 (1980).

[6] J. J. Pluth and J. V. Smith, "Crystal structure of dehydrated Ca-exchanged zeolite A. Absence of near-zero-coordinate Ca^{2+}. Presence of Al complex", *J. Am. Chem. Soc.*, **105**, 1192 (1983).

[7] S. B. Jang, Y. W. Han, D. S. Kim and Y. Kim, "The structures of dehydrated fully Ca^{2+}-exchanged zeolite A and of its iodine sorption complex", *Kor. J. Crystal.*, **1**, 76 (1990).

[8] V. Gramlich and W. M. Meier, "The crystal structure of hydrated NaA: a detailed refinement of a pseudosymmetric zeolite structure", *Z. Kristallogr.*, **133**, 134 (1971).

[9] L. B. McCusker and K. Seff, "The crystal structure of vacuum-dehydrated fully ammonium-exchanged zeolite A", *J. Am. Chem. Soc.*, **103**, 3441 (1981).

[10] V. Subramanian and K. Seff, "Crystal structure of dehydrated Cs and Tl-exchanged zeolite-A", *J. Phys. Chem.*, **83**, 2166 (1979).

[11] J. M. Shin, K. T. No and M. S. Jhon, "Molecular dynamics study on the Na ions bound in A-type zeolite framework", *J. Phys. Chem.*, **92**, 4533 (1988).

[12] M. Sprik, R. W. Impey and M. L. Klein, "Study of electron solvation in liquid ammonia using quantum path integral Monte Carlo calculations", *J. Chem. Phys.*, **83**, 5802 (1985).

[13] E. Huheey, "The electron negativities of groups", *J. Phys. Chem.*, **69**, 3284 (1965).

[14] R. T. Sanderson, *Chemical Periodicity* (Reinhold, New York, 1960).

[15] K. T. No, J. S. Kim, Y. Y. Huh, W. K. Kim and M. S. Jhon, "Intraframework potential energy function of zeolites. 1. $(T_2O_4Na)_n$-type Na-A zeolite", *J. Phys. Chem.*, **91**, 740 (1987).

[16] R. Y. Yanagida, A. A. Amaro and K. Seff, "A redetermination of the crystal structure of dehydrated zeolite 4A", *J. Phys. Chem.*, **77**, 805 (1973).

[17] M. D. Baker, J. Godber and G. A. Ozin, "Watching silver clusters grow in zeolites: direct probe Fourier transform-far-IR spectroscopy of the red form of fully silver ion-exchanged zeolite-A", *J. Phys. Chem.*, **89**, 2299 (1985).

[18] G. A. Ozin, M. D. Baker and J. Godber, "Crystal-field effects on the far-IR cation vibrations of transition metal (2+) ion exchanged faujasite zeolites" *J. Am. Chem. Soc.*, **107**, 1995 (1985).

[19] M. D. Baker, J. Godber and G. A. Ozin, "Frequency and intensity consideration in the far-IR spectroscopy of faujasite zeolites: experiment and theory. Metal cation vibrational assignments, site locations, and populations", *J. Am. Chem. Soc.*, **107**, 3033 (1985).

[20] G. Schrimpf, M. Schlenkrich, J. Brickmann and P. Bopp, "Molecular dynamics simulation of zeolite NaY. A study of structure, dynamics, and thermalization of sorbates", *J. Phys. Chem.*, **96**, 7404 (1992).

[21] D. J. Evans, W. G. Hoover, B. H. Failor, B. Moran, and A. J. C. Ladd, "Nonequilibrium molecular dynamics via Gauss's principle of least constraint", *Phys. Rev. A.*, **28**, 1016 (1983); A.D. Simmons and P. T. Cummings, "Nonequilibrium molecular dynamics simulation of dense fluid methane", *Chem. Phys. Lett.*, **129**, 92 (1986).

[22] C. W. Gear, *Numerical initial value problems in ordinary differential equation* (Englewood Cliffs NJ: Prentice-Hall, 1971).

[23] D. J. Evans, "On the representation of orientation space", *Mol. Phys.*, **34**, 317 (1977); D. J. Evans and S. Murad, "Singularity free algorithm for molecular dynamics simulation of rigid polyatomics", *ibid.*, **34**, 327 (1977).

[24] P. T. Cummings and T. L. Varner, Jr., "Nonequilibrium molecular dynamics calculation of the shear viscosity of liquid water", *J. Chem. Phys.*, **89**, 6391 (1988).

[25] C. K. Johnson, "ORTEP-II: A fortran thermal-ellipsoid plot program for crystal structure illustrations", Report ORNL-5138 (3rd revision of ORNL-3794, 1976), Oak Ridge National Laboratory, Oak Ridge, Tennessee.

[26] M. Neumann, "Dielectric relaxation in water. Computer simulations with the TIP4P potential" *J. Chem. Phys.*, **85**, 1567 (1986).

[27] S. H. Lee and P. J. Rossky, "A comparison of the structure and dynamics of liquid water at hydrophobic and hydrophilic surfaces – a molecular dynamics simulation study", *J. Chem. Phys.*, **100**, 3334 (1994).

[28] S. H. Lee and J. C. Rasaiah, "Molecular dynamics simulation of ionic mobility. I. Alkali metal cations in water at 25°C", *J. Chem. Phys.*, **101**, 6964 (1994).